Journal of the Korean Society for Nondestructive Testing
Vol. 27, No. 3 (2007. 6)

The Scanning Laser Source Technique for Detection of Surface-Breaking and Subsurface Defect

Younghoon Sohn*,† and Sridhar Krishnaswamy**

Abstract The scanning laser source (SLS) technique is a promising new laser ultrasonic tool for the detection of small surface-breaking defects. The SLS approach is based on monitoring the changes in laser-generated ultrasound as a laser source is scanned over a defect. Changes in amplitude and frequency content are observed for ultrasound generated by the laser over uniform and defective areas. The SLS technique uses a point or a short line-focused high-power laser beam which is swept across the test specimen surface and passes over surface-breaking or subsurface flaws. The ultrasonic signal that arrives at the Rayleigh wave speed is monitored as the SLS is scanned. It is found that the amplitude and frequency of the measured ultrasonic signal have specific variations when the laser source approaches, passes over and moves behind the defect. In this paper, the setup for SLS experiments with full B-scan capability is described and SLS signatures from small surface-breaking and subsurface flaws are discussed using a point or short line focused laser source.

Keywords: Scanning Laser Source Technique, Surface-Breaking Defect, Subsurface Defect

1. Introduction

As originally developed by Kromine et al. (2000), the SLS technique offers several advantages over conventional ultrasonic flaw detection techniques (Sohn and Krishnaswamy, 2004). All the advantages of laser based ultrasonics including non-contact and curved surface inspection apply to the SLS approach as well. In addition, SLS offers the following features:

- Ease of scanning: Conventional ultrasonic generators such as contact piezoelectric-transducers (PZT) and near-contact electro-magnetic acoustic transducers (EMATs) are not as easily scanned as a laser beam.
- High resolution for detection of small defects: For investigation of small anomalies in a structure, a narrow ultrasonic source may be essential in some applications. Conventional methods may not provide a sufficiently narrow ultrasonic source.
- Detection of defects with arbitrary orientation: The SLS technique can be used to detect defects of various orientations with respect to the scanning direction. This is because the SLS technique is not as sensitive as pulse-echo techniques to the orientation of the crack with respect to the generating/receiving transducer. This feature increases the probability of detection as compared with a conventional pitch-catch or pulse-echo approach.
- Coupling independence: The detection of the generated ultrasound is done at a fixed

Received: April 29, 2007, Accepted: May 25, 2007. * Samsung Electronics CO., LTD., Manufacturing Technology Team 1, Memory Division, Semiconductor Business, San #16, Banwol-dong, Hwasung-city, Gyeonggi-do, 445-701, Korea, ** Center for Quality Engineering and Failure Prevention, Northwestern University, 2137 Tech Drive, Evanston, IL 60208-3020, USA, † Corresponding author: yh.sohn@samsung.com

location and can be monitored using either a laser interferometer or a contact PZT-transducer. The laser interferometer provides non-contact absolute measurements, and a PZT-detector provides higher sensitivity, and therefore this choice can be determined by the application condition. In either case, since the detection is at a fixed location, variability associated with PZT-coupling or laser speckle for interferometric detection is eliminated.

- Signal to noise improvement: The SLS approach provides enhanced signal to noise performance compared to conventional pitch-catch mode of operation. This is because the presence of an anomaly is indicated by an increase in the amplitude of the detected ultrasonic signal rather than by the presence of a weak echo, and by variations of the ultrasonic frequency when the SLS is in the vicinity of a discontinuity. Furthermore, when laser-based techniques such as the SLS use a fairly large generation source, it has been noted that they are less sensitive to grain noise, thereby enabling detection of small fatigue cracks (Yan and Nagy, 2002).

2. SLS Technique for Detection of Surface-Breaking Defects

2.1 Experimental Setup of SLS

The major components of experimental apparatus are indicated schematically in Fig. 1. Surface acoustic waves (Rayleigh waves) are generated using a pulsed Nd:YAG laser of 1064 nm wavelength. The generating laser beam is piped to the specimen using a 200 μm diameter optical fiber. The incident energy level is kept low enough to avoid damaging the specimen in this case. The laser beam is focused by a cylindrical lens into short line of 5 mm length and 250 μm width (full width of the Gaussian at half the maximum) approximately within an error of a few tens of microns. The movement of the fiber tip is controlled by a stepper motor which is connected to a PC. The minimum step size of the stepper is 5 μm.

The surface wave generated in the manner described above is detected using a He-Ne Michelson interferometer equipped with a stabilization circuit. The interferometer whose beam is focused by a spherical lens as a small spot is adapted for measurement of ultrasonic displacement with 1 ~ 15 MHz bandwidth. The geometric details (size of scan and defect) are shown in Fig. 2. A titanium (Ti-6Al-4V) specimen with a surface-breaking EDM notch of 1 mm length, 50 μm width, and 500 μm depth is used for the SLS experiment. The scanning size is 3.9 mm (78 scans with 50 μm step size) and the ultrasound receiver is fixed at a distance of 4.5 mm from the first scanning position.

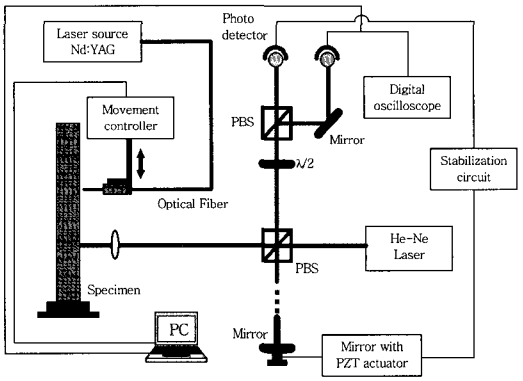

Fig. 1 Schematic of experimental setup. Laser source is focused as a short line and the detection interferometry beam is a spot. (PBS: polarizing beamspliter, λ/2: half-wave-plate)

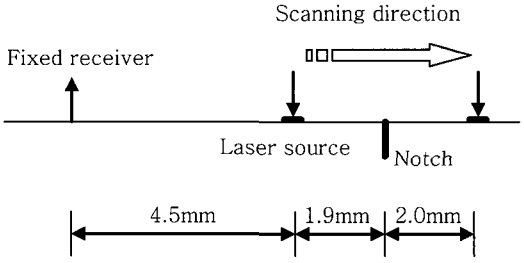

Fig. 2 Experimental schematic of SLS and surface-breaking EDM notch of 1 mm length, 50 μm width, and 500 μm depth on a titanium specimen.

2.2 SLS Amplitude Signature (B-scan)

B-scan results of the ultrasonic amplitude of the generated signal versus the SLS position as it was scanned over the notch is shown in Fig. 3. The SLS position is defined as the distance between the source position of the first scanning source and the center position of each scanning source. Each horizontal line in the B-scan represents the corresponding time domain ultrasonic displacement as a gray level. Distinct propagating waves can be seen in the B-scans. The tangent of the lines of the propagating waves in a B-scan represents the speed of the corresponding waves. When the laser source is far ahead of the defect, the direct and defect-reflected Rayleigh waves can be seen in the time interval and they get closer as the source approaches the defect. Also, scattered longitudinal waves generated by the Rayleigh wave propagating and interacting with the defect can be seen. When the laser source passes over the surface-breaking defect, significant amplitude and spectral changes occur in the signal expected at the direct Rayleigh wave arrival time. As the laser source approaches the defect, the signal amplitude significantly increases and as the source passes behind the defect, the signal amplitude decreases due to screening by the defect. Far away from the flaw, some portion of the ultrasonic energy remains and even increases a little as a portion of the incident wave passes around the defect due to diffraction.

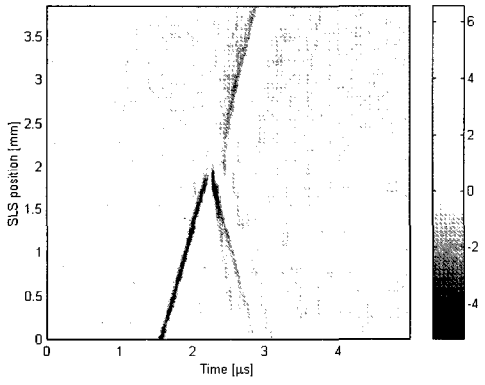

Fig. 3 B-scan result of ultrasound amplitude for the surface-breaking defect.

2.3 SLS Peak-to-Peak Signature

The SLS B-scans provide a broad picture of the interaction of the SLS with the defect. Clearer indication of defect location can be obtained by comparing the amplitudes of the direct Rayleigh wave arrivals for different SLS positions. Ultrasonic time domain signals at typical SLS positions are shown in Fig. 4. It is seen that the short line source generates a bipolar Rayleigh wave. The following aspects of the signal (around a gate windowed at the Rayleigh-wave arrival) should be noted:

- In the absence of a defect or when the source is far ahead of the defect, the signal is of sufficient amplitude above the noise floor to be easily measured by the laser detector (Fig. 4 (a)).
- As the source approaches the defect, the amplitude of the detected Rayleigh-wave signal significantly increases (Fig. 4 (b)). This increase is readily detectable even with a low sensitivity laser interferometer as compared to weak echoes from the flaw. The variation in signal amplitude is due to two mechanisms: (1) interaction of the direct ultrasonic wave with the waves scattered by the defect, and (2) changes in the conditions of generation of ultrasound when the SLS is in the vicinity of the defect.
- As the source moves behind the defect (Fig. 4 (c)), the amplitude drops lower than in Fig. 4 (a) due to scattering of the generated signal by the defect.

Plots of the peak-to-peak amplitude of the Rayleigh wave signal versus the SLS position are shown in Fig. 5. All data are normalized to peak-to-peak value of incident Rayleigh waves far ahead of the crack. When the source is far ahead of the defect (region A) the dominant waves are incident waves which directly

propagate to the receiver without interacting with the defect (the reflected waves which arrive later are relatively smaller than the incident waves, Fig. 4 (a). Thus the peak-to-peak amplitudes or vertical displacements show stable behavior and are seen to be the same as in the absence of a crack. As the source approaches and is over the crack, a significant increase of peak-to-peak signals occurs (region B) and in fact reaches its maximum when the center of the source is located just ahead of the defect. Since the energy of laser source has a Gaussian distribution, the greatest portion of the energy is at center of the source. Thus it is reasonable that the maximum occurs when the center of the source is just ahead of the defect since in this case the surface waves having the highest portion of energy are generated and these interact with the defect. As the source passes over the crack the amplitude decreases noticeably and becomes stable when the source is far behind the defect (region C). Note that, though the defect depth (500 μm) is of comparable size to the center wavelength of the surface wave generated (750 μm), a significant portion of the incident energy passes around the defect because the surface-breaking defect is short in this experiment compared to the wavelength.

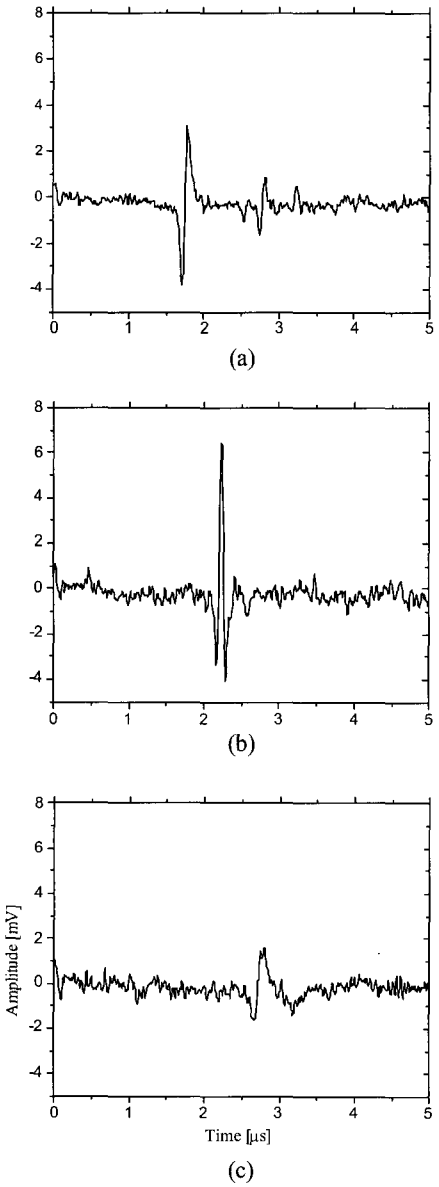

Fig. 4 Representative ultrasonic time domain signals detected by the interferometer when the laser source is: (a) far ahead, (b) close to, and (c) behind the surface-breaking defect.

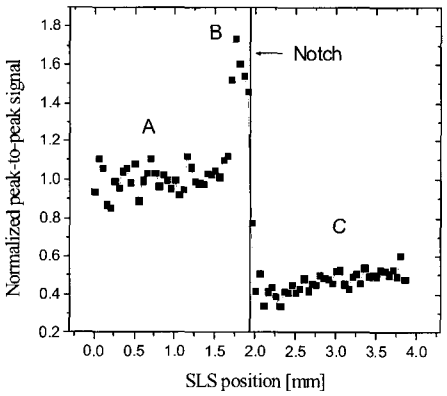

Fig. 5 Peak-to-peak signal versus SLS position. All data are normalized by the peak-to-peak value of incident Rayleigh waves.

2.4 SLS Spectral Signature

Characteristic spectral changes of the SLS signal are also observed in the experiment. In particular, it is found that the maximum frequency increases and subsequently decreases as the SLS scans a surface-breaking crack (Fig. 6). The spectral contents of the signals (window-

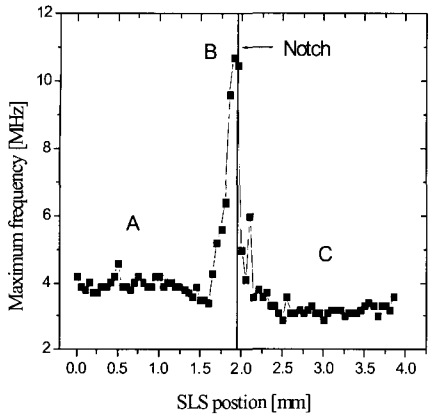

Fig. 6 Maximum frequency versus SLS position. The spectral content of the signals are obtained using FFT after window gating the signals around the direct Rayleigh wave arrival.

gated around the direct Rayleigh wave arrival) are obtained using standard FFT processing. When the source is far ahead of the defect (region A), as one would expect, the maximum frequency (4 MHz) is the same as that of the Rayleigh wave in the absence of any cracks. The maximum frequency of surface waves generated by a laser source is inversely related to the width of the laser source (Huang et al., 1992; Berthelot and Jarzynski, 1990). When the SLS straddles the defect, the effective width of the laser source is reduced and this causes a shift to higher frequencies (region B). When the SLS is behind the defect (region C), the maximum frequencies drop and become stable. This is also expected from the fact that higher frequency components of the generated wave are better screened by the crack than lower frequency components corresponding to the defect size. Note that the difference in maximum frequency between region A (far ahead) and C (far behind) is not very large.

3. SLS Technique for Detection of Subsurface Defects

One of the most important advantages of ultrasonic testing (UT) is that UT makes it possible to investigate anomalies below the material surface. The question that we will address next is whether the SLS technique can be applied for detection of subsurface defects. Clearly, in this case there is no direct interaction of the generation source with the flaw. Rather, the SLS technique in this case is essentially a pitch-catch UT technique, with the primary advantage being the ease with which laser sources can be scanned.

Fig. 7 shows a schematic of the SLS technique applied to the detection of subsurface defects. In general, the scattered ultrasound caused by interference with subsurface defects can be expected to exhibit complicated behavior. For instance, Lamb wave modes may be excited as the SLS is directly over a near subsurface defect. Furthermore, these Lamb waves can also be excited by incoming Rayleigh waves even when the ultrasound source is far away from the defect (Clark et al., 2000). The question that is of interest is whether an analysis of the scattered ultrasound can be used to determine both the width and the depth of the subsurface defect.

3.1 Experimental Setup of SLS

The components of the experimental setup for generation and detection of ultrasound are basically the same as in the case of surface-breaking defect detection. The energy of the incident source is sufficiently low for thermoelastic generation of ultrasound. The frequency of the generated Rayleigh waves on a flawless structure is found to be 2.5 ~ 2.8 MHz. Fig. 7 shows the shape of defect and the scanning direction which is perpendicular to the defect. Experiments were performed on a thick aluminum plate with various defect sizes. The geometries used for the subsurface flaw were: 1) 1.6 mm width at a 100 μm depth, 2) 3.2 mm width at a 100 μm depth, and 3) 1.6 mm width at a 200 μm depth. The scanning length was 9 mm with 60 μm step size.

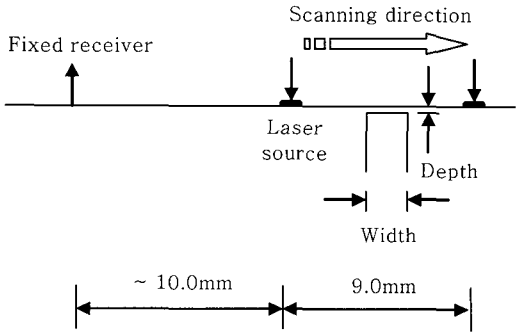

Fig. 7 Schematic of the SLS technique applied to the detection of rectangular subsurface defects (1.6 mm width at a 100 μm depth, 3.2 mm width at a 100 μm depth, and 1.6 mm width at a 200 μm depth.)

3.2 SLS amplitude signature (B-scan)

Experimental B-scan results of the ultrasonic amplitude (mV) versus the SLS position are shown in Fig. 8. In Fig. 8 (b), amplitudes are normalized by the maximum value of each stage of scan in order to better visualize the various waves present (irrespective of their amplitude). The defect width in this case is 1.6 mm and the depth is 100 μm (with an error of a few tens of micrometers due to the accuracy of traditional milling machines).

When the laser source is far ahead of the defect, the incident and reflected Rayleigh waves can be seen in the time interval and they get closer as the source approaches the defect. When the source is just on one edge of the defect, reverberating signals which last for quite a while start to be generated. The generation of these reverberating signals ceases when the source just passes over the other edge of the defect. A time trace signal when the source is in the middle of the defect (corresponding to the dashed line in the B-scan) is shown in Fig. 9. The frequency of the trailing bouncing signal is found to be 1.70 MHz for this case.

It should be possible to relate the frequency of the reverberating signals to either the width or the depth of the flaw. Because bulk (shear

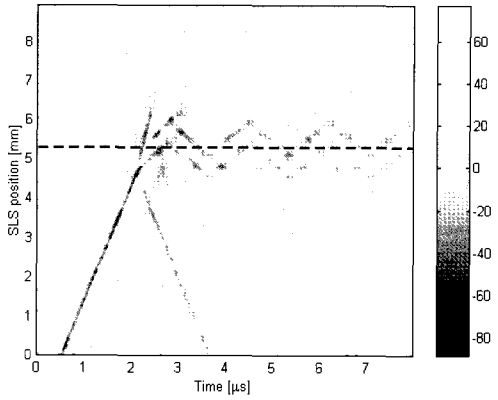

(a) B-scan image in mV

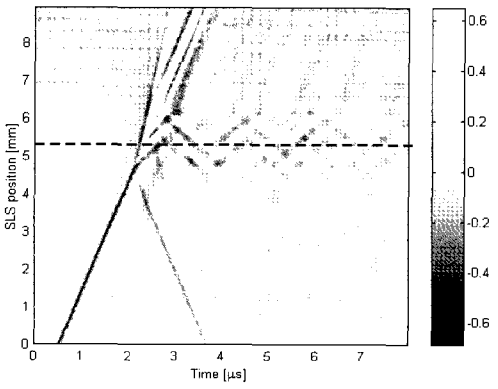

(b) Normalized B-scan image

Fig. 8 B-scan result for subsurface defect of 1.6 mm width at a 100 μm depth. The amplitudes are normalized by the maximum value of each stage of scan in (b).

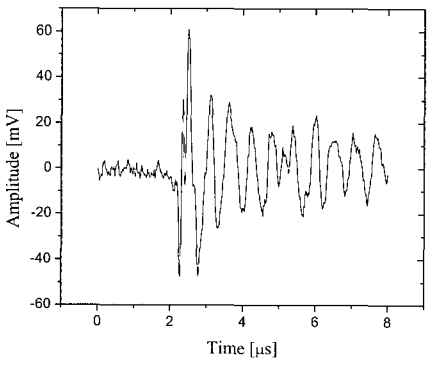

Fig. 9 A time trace signal when the source is in the middle of the defect (dashed line on Fig. 8). The frequency of the reverberating signal is found to be 1.70 MHz.

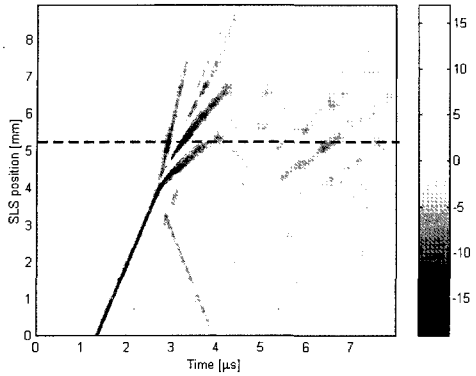

(a) B-scan image

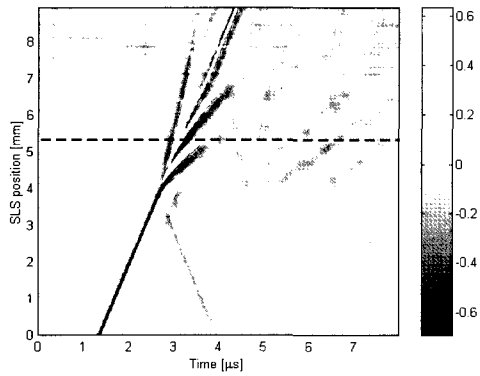

(b) Normalized B-scan image

Fig. 10 Experimental B-scan for subsurface defect of 3.2 mm width at a 100 μm depth. The amplitudes are normalized by the maximum value of each stage of scan in (b).

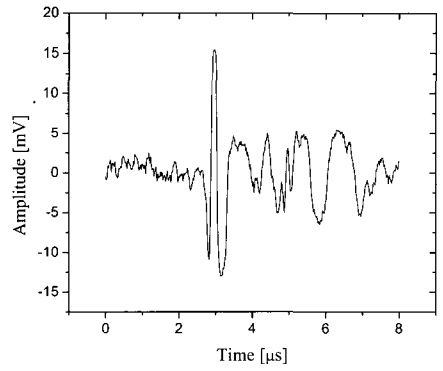

Fig. 11 A time trace signal when the source is in the middle of the defect (dashed line on Fig. 10). The frequency of the reverberating signal is found to be 0.86 MHz.

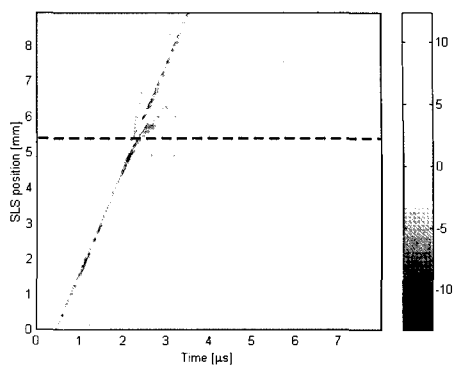

(a) B-scan image

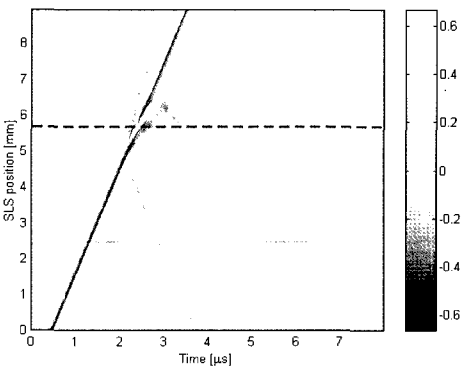

(b) Normalized B-scan image

Fig. 12 Experimental B-scan for subsurface defect of 1.6 mm width at a 200 μm depth. The amplitudes are normalized by the maximum value of each stage of scan in (b).

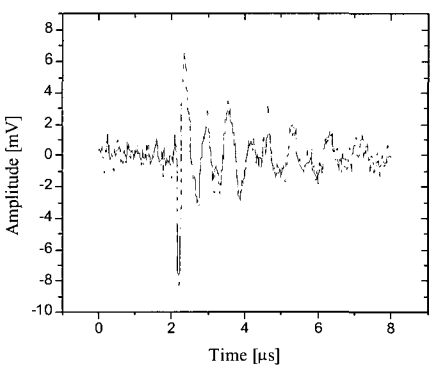

Fig. 13 A time trace signal when the source is in the middle of the defect (dashed line on Fig. 12). The frequency of the reverberating signal is found to be 1.66 MHz.

and longitudinal) waves propagate into the material, one source of the reverberating signals could be due to reflections between the free top surface and the subsurface defect. This reverberating signal should be of very high frequency range (16 ~ 30 MHz) for a flaw depth of 100 μm thickness. However, it is not possible to detect such high frequencies with the current detection system setup, and therefore these high frequency bounces are not seen in the experiment. To see if the reverberating frequency was related to the width of the flaw, another set of experiments was performed with a defect of a wider width (3.2 mm) but the same thickness (100 μm) of defect. B-scan signatures for this case are shown in Fig. 10. The wider width of the defect can be clearly seen in the B-scan and the overall general signature is the same as in the previous result. The frequency of the reverberating signal however decreased to 0.86 MHz (Fig. 11). In third experiment (Fig. 12), where the defect width is 1.6 mm and depth is 200 μm, the amplitude of the reverberating signal is reduced but its frequency rises to 1.66 MHz which is reasonably close to the first case (Fig. 13). It therefore appears that the reverberating frequency is related to reflections of waves from either end of the flaw, and therefore is related to the width of the flaw. To measure the depth of the flaw, it might be necessary to increase the photo-acoustic detection bandwidth to at least a few tens of MHz as well as its sensitivity in order to monitor reflections of bulk longitudinal and shear waves between the top surface and the defect.

4. Conclusion

In this paper, the SLS technique is demonstrated experimentally for detection of surface-breaking and subsurface defect. SLS experiments were done using full photo-acoustic system, i.e. a Q-switched Nd:YAG laser as the source and a He-Ne Michelson interferometer as the detector. The laser source is focused on a relatively small region of 5 mm length and ~ 250 μm width. As the SLS scans over a flaw, characteristic changes are observed in the Rayleigh and reverberating wave signal. Experimentally, it has been shown that the SLS technique provides distinct flaw signatures for small defects on material surfaces as well as for rectangular defects slightly below the surface. The B-scans provide a broad picture of the interaction of the SLS with the defect. Clearer indication of defect location can be obtained by comparing the peak-to-peak amplitudes of the direct Rayleigh wave arrivals for different SLS positions and their frequency contents. In the case of subsurface defect, it is found that the frequency of reverberating signals is related to defect size, especially the width of the flaw. In summary, this paper demonstrates that both surface-breaking and subsurface flaw could be detected effectively by using SLS technique.

References

Berthelot, Y. H. and Jarzynski, J. (1990) Directional Laser Generation and Detection of Ultrasound with Arrays of Optical Fibers, *Review of Progress in QNDE*, Vol. 9, eds. D. O. Thompson and D. E. Chimenti, American Institute of Physics, New York, pp. 463

Clark, Matt, Sharples, Steve and Somekh, Mike (2000) Non-Contact Acoustic Microscopy, Meas. Sci. Technol. Vol. 11, pp. 1792-1801

Huang, J., Krishnaswamy, S. and Achenbach, J. D. (1992) Laser Generation of Narrow-Band Surface Waves, J. Acoust. Soc. Am. Vol. 92 (5), pp. 2527-2531

Kromine, A. K., Fomitchov, P. A., Krishnaswamy, S. and Achenbach, J. D. (2000) Laser Ultrasonic Detection of Ssurface Breaking Discontinuities: Scanning Laser Source Technique, Material

Evaluation, Vol. 58, No. 2, pp. 173-177

Sohn, Y. and Krishnaswamy, S. (2004) Interaction of a Scanning Laser-Generated Ultrasonic Line Source with a Surface-Breaking Flaw, Journal of Acoustic Society of America, Vol. 115, No. 1, pp. 172-181

Yan, Z. and Nagy, P. B. (2002) Enhanced Laser Generation of Surface Acoustic Waves by Discontinuities, *Review of Progress in QNDE*, Vol. 20, eds. D.O. Thompson and D.E. Chimenti, American Institute of Physics, New York, pp. 204-211